3 Surfaces and Interfaces

3-1 Si(111)-6×1(3×1)-Ag Surface Structure Investigated by X-ray Crystal Truncation Rod Scattering

The Si(111)-6×1-Ag surface is a superstructure induced by a submonolayer of silver atoms on the Si(111) substrate, and has many interesting features, including its temperature-related phase changes. The 6×1 structure shown at room temperature changes to a 3×1 structure above 500 K [1]. Moreover, it was found from a low-energy electron diffraction (LEED) observation that the surface takes a c(12×2) structure below 100 K [2].

Another feature of the Si(111)-6×1-Ag surface is the low-dimensional structure of the surface atoms. According to most of the previously suggested structure models the Ag and reconstructed Si atoms form one-dimensional rows. The precise arrangement of the surface atoms, however, has not yet been determined. Information on this structure is important for the understanding of surface properties such as kinetics, electric features, and phase transitions.

In this study, we observed the X-ray scattering intensities along the crystal truncation rod (CTR), with emphasis on the 00 rod in order to analyze the perpendicular structure of the Si(111)-6×1-Ag surface. The measurement was performed at BL-15B2, where a six-circle diffractometer with the ultra-high vacuum chamber is installed. In-situ X-ray diffraction measurements can be performed with this equipment.

The observed intensities are shown in Fig. 1. The reciprocal points of $\ell = 3$ and 9 correspond to the 111 and 333 Bragg points in Miller indices. Around the Bragg points, the intensities show strong asymmetries. This can be explained as being due to the interference between

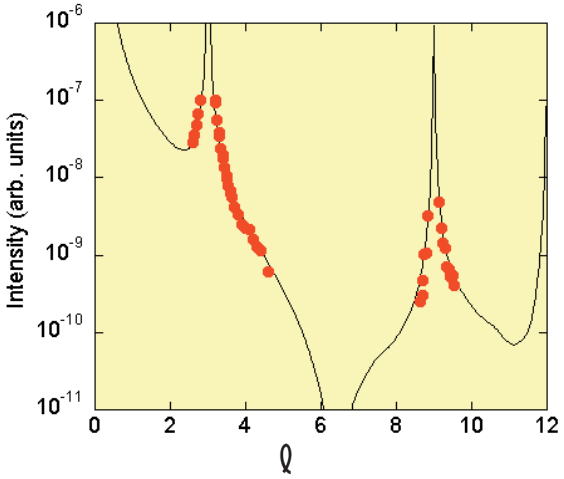

Figure 1
Observed CTR scattering intensities along the 00 rod. The solid line indicates the calculated profile using the fitted parameters.

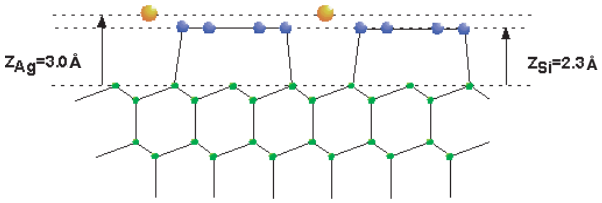

Figure 2
Side view of the Si(111)-6×1-Ag surface structure determined by the fitting procedure.

scattering waves from the surface atoms and from the substrate, indicating that the measurement is sensitive to the surface structure. Intensities in the range of $4 < \ell < 8$ were too weak to be obtained.

Least-squares fitting analyses were used for the determination of the atomic arrangement perpendicular to the surface. In the analyses, we constructed structure models consisting of at most two layers of reconstructed Si atoms, with the assumption that the 6×1 structure is composed of two equivalent 3×1 structures. The number and the distribution of the Si atoms were changed; the results were compared with each other. As a result, the best-fitted model shown in Fig. 2 was obtained. In this model four Si atoms lie on a single layer between the surface Ag layer and the substrate. The heights of the Ag and Si atoms are 3.04±0.01 Å and 2.31±0.01 Å. The *R*-factor, which indicates the goodness of fit, is 0.094. The calculated intensities using this model are shown in Fig. 1 and reproduce well the asymmetry around the Bragg points. The structure determined in this study is consistent with the honeycomb-chain-channel (HCC) model proposed for the alkali-metal induced 3×1 structure [3].

The Si(111)-6×1-Ag surface is produced by the desorption of Ag atoms from the Si(111)-√3×√3-Ag surface. The heights of the Ag and Si atoms on the Si(111)-√3×√3-Ag surface are 3.05 Å and 2.26 Å [4]. We have thus found that the heights of both the Ag and the reconstructed Si atoms are quite similar for the two surfaces, suggesting that the position of the surface atoms does not change during the desorption of Ag atoms.

K. Sumitani[1], K. Masuzawa[1], T. Hoshino[1], S. Nakatani[1], T. Takahashi[1], H. Tajiri[2], K. Akimoto[3], H. Sugiyama[4], X.-W. Zhang[4] and H. Kawata[4] ([1]Univ. of Tokyo, [2]JASRI, [3]Nagoya Univ., [4]KEK-PF)

References

[1] Y. Gotoh and S. Ino, *Jpn. J. Appl. Phys.*, **17** (1978) 2097.
[2] K. Sakamoto, H. Ashima, H. M. Zhang and R. I. G. Uhrberg, *Phys. Rev. B,* **65** (2001) 045305.
[3] S. C. Erwin and H. H. Weitering, *Phys. Rev. Lett.*, **81** (1998) 2296.
[4] T. Takahashi and S. Nakatani, *Surf. Sci.*, **282** (1993) 17.

3-2 Fabrication of a One-dimensional Ordered Structure of α-sexithienyl on Ag(110) and Cu(110)

Organic materials are widely applied for various electronic devices, such as organic electroluminescences and field-effect transistors. The characteristics of these devices are strongly dependent on the energy level alignment at the organic/metal interface, and the energy level alignment is dominated by the atomic structures at the interface. It is therefore important to be able to control the atomic structure and to fabricate well-defined nano-structures [1]. In the present study, we have tried to prepare a 1D structure of α-sexithienyl (6T) on a metal substrate [2,3]. 6T is one of the most promising π-conjugated organic materials.

6T molecules were evaporated on Ag(110) and Cu(110) using a Knudsen cell, and near-edge X-ray absorption fine structure (NEXAFS) measurements at the S K-edge were carried out at BL-11B.

Fig. 3 (a) shows the polarization (θ) dependent NEXAFS of a 4 Å thick 6T film on Ag(110). Peak 1 at 2472.4 eV is assigned to the S 1s-to-π* transition and its transition moment is normal to the molecular plane, while peak 2 at 2473.3 eV is assigned to the S 1s-to-σ* (S-C) transition, and its moment is parallel to the molecular long axis. The intensity of peak 2 is higher at the normal X-ray incidence (90°), indicating that 6T grew with its molecular long axis parallel to the surface. Fig. 3 (b) shows the azimuthal (φ) dependent NEXAFS recorded at normal X-ray incidence. In the figure, 0° and 90° are defined as the Ag [1$\bar{1}$0] and [001] directions. Fig. 4 (a) shows the intensity of the σ* peak as a function of azimuthal angle. The intensity of the σ* peak is strongest at 90° and weakest at 0°, showing that the molecular long axis is parallel to the Ag[001] direction. The polarization and azimuthal dependent NEXAFS results indicate that we were successful in fabricating a 1D ordered structure of 6T on Ag and Cu(110) (see Fig. 4 (b)).

It should be noticed that the molecular orientation of 6T can be directly determined by the azimuthal dependence NEXAFS. Here, we propose a new method to obtain the orientation distribution function of molecules with twofold symmetry. The orientation distribution function is approximated by the Gaussian function

$$f(\varphi)=\frac{1}{\sqrt{2\pi\sigma}}e^{-\frac{(\varphi-\pi/2)^2}{2\sigma^2}},$$

where σ^2 is the dispersion. The intensity of the NEXAFS peak is proportional to $\cos^2\alpha$, where α is the angle between the electric vector of the X-ray and the transition moment of the peak. The intensity of the σ* peak observed by NEXAFS can thus represented as

$$I(\beta)=\int_0^{2\pi} f(\varphi)\cos^2(\beta-\varphi)\,d\varphi,$$

where β is the azimuthal angle between the electric vector of incident X-ray and the [1$\bar{1}$0] direction. By fitting the experimental results with this function, σ was determined to be 29° for 6T/Cu(110) and 18° for 6T/Ag(110). σ is smaller for 6T/Ag(110), indicating that a more ordered 1D structure of 6T is formed on Ag(110). Fig. 4 (c) shows the obtained orientation distribution function ($f(\varphi)$) of 6T on Cu(110) and Ag(110).

In conclusion, we have successfully fabricated 1D structures of 6T on Ag and Cu(110), and proposed a new method to obtain the orientation distribution function of molecules using NEXAFS.

M. Kiguchi[1], G. Yoshikawa[2], S. Entani[2], S. Ikeda[2] and K. Saiki[2] ([1]Hokkaido Univ., [2]Univ. of Tokyo)

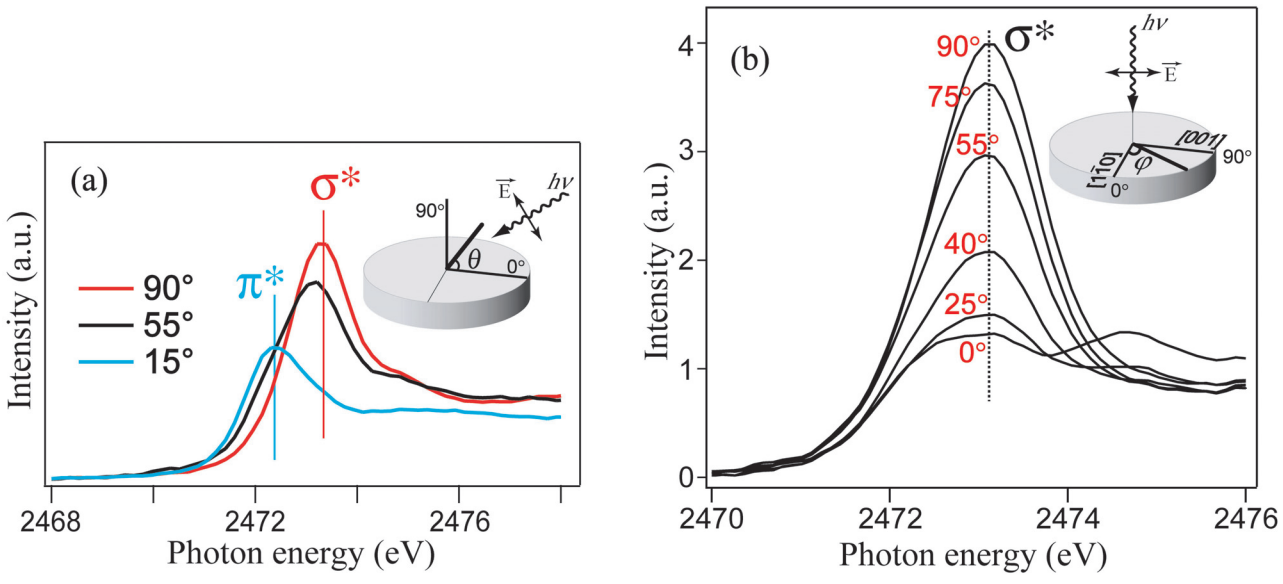

Figure 3
(a) The polarization (θ) dependent NEXAFS of 4 Å thick 6T/Ag(110), (b) Azimuthal (φ) dependent NEXAFS taken at normal X-ray incidence.

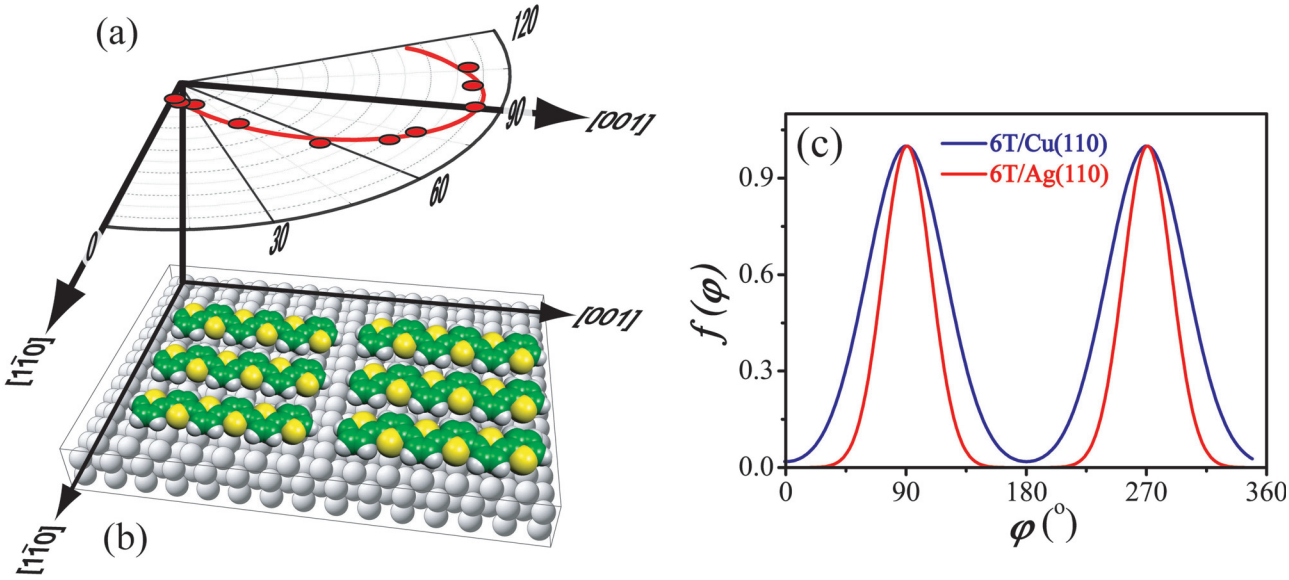

Figure 4
(a) Polar plot of σ*-peak intensity as a function of φ, (b) The schematic model of 1 ML thick 6T on Ag(110). (c) The orientation distribution function of 6T molecules on Ag(110) and Cu(110).

References

[1] M. Kiguchi, S. Entani, K. Saiki and G. Yoshikawa, *Appl. Phys. Lett.,* **84** (2004) 3444.
[2] G. Yoshikawa, M. Kiguchi, S. Ikeda and K. Saiki, *Surf. Sci.,* **559** (2004) 77.
[3] M. Kiguchi, G. Yoshikawa and K. Saiki, *J. Appl. Phys.* **94** (2003) 4866.

3-3 Change of Molecular Packing and Orientation from Monolayer to Multilayers of Hydrogenated and Fluorinated Carboxylate Studied by in-plane X-ray Diffraction Together with NEXAFS Spectroscopy at the C K-edge

Functionalized amphiphiles are expected to have future applications as electronic- and/or optical-devices in the form of organized molecular films, having the advantages of characteristics variable with chemical modification, and their potential for ordered fabrication at the nano-scale as well as molecular construction combined with inorganic materials. In the present work, the molecular alignments in LB films of hydrogenated and fluorinated long-chain carboxylates are investigated by in-plane X-ray diffraction (XRD) and NEXAFS spectroscopy. This analysis is used to obtain the molecular arrangements in the two-dimensional film planes of amphiphiles both in monolayer form and as multilayer films on solids, providing important information on the standard molecular lattice packing in the films.

Monolayers of stearic acid dissolved in benzene and perfluorostearic acid dissolved in a mixed solvent of $CHCl_3$:CF_3COOH (4:1 v/v) were spread on to an aqueous buffer solution containing $CdCl_2$ and $KHCO_3$ (pH = 6.8). These monolayers were transferred onto solids at 15°C with the LB method at 25 mNm^{-1} to obtain alternating Y-type films. The long-spacing of the layer structures were measured using an X-ray diffractometer equipped with a graphite monochromator, and an in-plane diffractometer with a parabolic graded multilayer mirror was used to measure the two-dimensional lattice spacing of the films. C K-edge NEXAFS spectra were recorded at BL-7A in the partial electron yield mode with –200 V retarding voltage under vacuum in the 10^{-8} Torr range.

Fig. 5 shows the out-of plane (a) and in-plane (b) XRD profiles of 3, 5, 7, and 9 monomolecular layers of cadmium stearate (CdC_{18}) deposited on glass. For the out-of-plane XRD profiles the first, second, third, and so on (n = 1, 2, 3, etc.) order reflections indicate a long spacing of the double layers of around 50 Å, mainly due to the repeating distance between the hydrophilic Cd^{2+} ion layers in the Y-type films. In order to reveal the structural changes in the two-dimensional sub-cell lattice from the monolayer to the built-up multilayers, the in-plane XRD of the CdC_{18} LB films has been measured, and is shown in Fig. 5(b). The CdC_{18} monolayer on glass exhibits only a single diffraction peak at d_1 = 4.1 Å, suggesting an isotropic hexagonal sub-cell packing of the rotational hydrocarbon chains. As the number of the layers is increased, another reflection of the short spacing at 3.7 Å appears alongside the 4.1 Å diffraction, suggesting the formation of an orthorhombic molecular packing with a slightly distorted lattice. Thus the two-dimensional lattice of the molecular packing in the CdC_{18} LB films appears to change from the first layer to the subsequently built-up multilayers.

By using NEXAFS spectroscopy, structural information of not only the two-dimensional molecular packing but

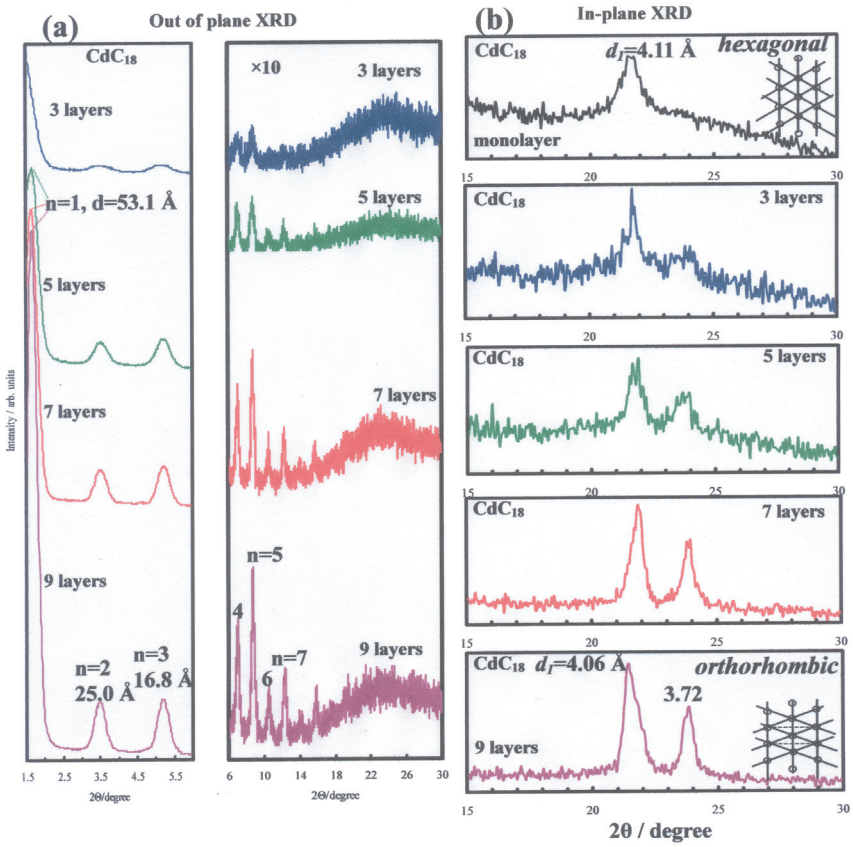

Figuer 5
(a) Out-of-plane XRD profiles of LB multilayers for cadmium stearate (3, 5, 7,and 9 layers). (b) In-plane XRD profiles of LB films for CdC_{18} (1, 3, 5, 7, and 9 layers).

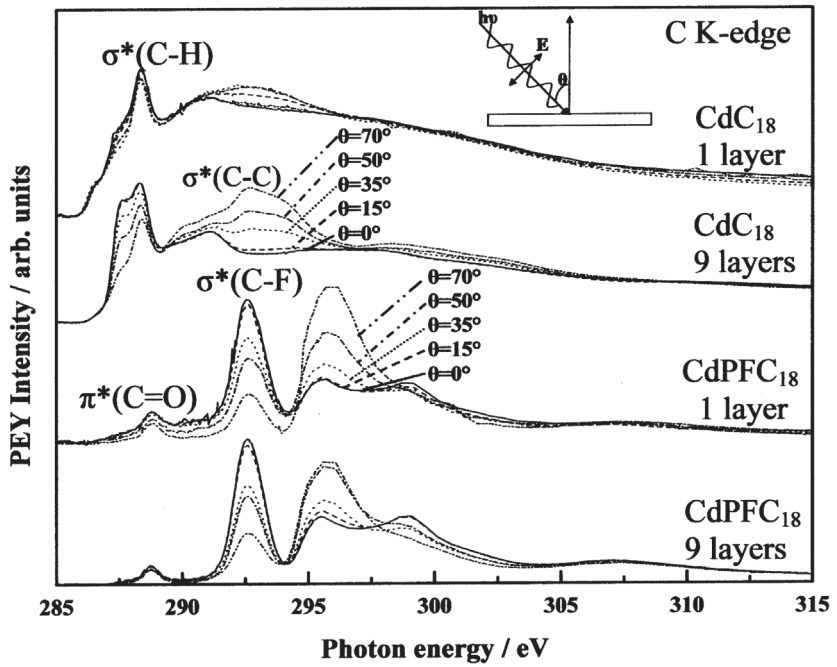

Figure 6
Polarized NEXAFS spectra of LB films for CdC_{18} and $CdPFC_{18}$ (1 and 9 layers) at the C K-edge.

also of the molecular ordering in the film plane could be obtained (Fig. 6). The dependence of C K-edge NEXAFS spectra on the number of layers was studied for CdC_{18} and cadmium perfluorostearate ($CdPFC_{18}$) films. From a Gaussian-function curve-fitting analysis to these spectra at the magic incidence angle (θ= 35°) for the CdC_{18} and $CdPFC_{18}$ 9 layers LB films, each observed band could be assigned to transitions from C 1s to π^*(C=O) at 287.6 eV, σ^*(C-H) at 288.4 eV, σ^*(C-F) at 292.6 eV, and σ^*(C-C) at 295.6 eV. For the CdC_{18} films, a change in dependence on the incident X-ray angle between the monolayer and 9-layer samples was clearly found, in particular for the C 1s-σ^*(C-H) and C 1s-σ^*(C-C) transition peaks. A similar dependence on the number of layers was not found at the C 1s-σ^*(C-F) transition for the $CdPFC_{18}$ films.

A. Fujimori[1], H. Nakahara[2], K. Seki[3] and Y. Ouchi[3], ([1]Yamagata Univ., [2]Saitama Univ., [3]Nagoya Univ.)

3-4 Condensation of Ions at a Surface Monolayer

The knowledge of the distribution of ions in the vicinity of a charged surface plays a key role in explaining electrochemical phenomena, colloid behavior, and ion-exchange reactions. The distribution depends on the charge density and chemical nature of the surface. Surface monolayers have advantages over other surfaces for these studies because these intrinsic properties can easily be varied. To assess the effects of the surface charge density on the ionic distribution, we have estimated the amount of ions at the solution surface by using the total-reflection total-conversion-helium ion yield (TRTCY) XAFS method [1]. An improved cell, shown in Fig. 7, has allowed us to record TRTCY-XAFS spectra of ions at a controlled surface area (surface pressure) by moving PTFE barriers [2-4]. The surface tension π can be measured using the Wilhelmy plate method. Unfortunately, the glass plate used in the Wilhelmy method deforms the flat and smooth solution surface (a grazing incidence angle is required in TRTCY-XAFS; typically 0.79 mrad in our measurements), so the XAFS and surface tension measurements were carried out separately. All of the XAFS spectra were recorded at BL-7C. A 30 μL aliquot of 1.0 mM di-hexadecyl-di-methyl-ammonium bromide (C16) solution in benzene was applied to the surface of a 10 mM KBr aqueous solution with a microsyringe. The area of covered by the C16 molecules on the surface *A* was changed from 180 to 50 Å^2 by membrane compression, and the amount of Br^- attracted by the C16 surface monolayer was estimated from the edge jump at the Br *K*-edge.

The difference in the condensation state of the surfactant influences the X-ray intensity reaching the solution surface. Part of the incident X-ray may be reflected at the upper surface of the surfactant membrane or at the aqueous solution surface (Fig. 8). The experimental plots shown in Fig. 9 take into account this damping effect. Two surface adsorption models were considered to explain the experimental data; the Gouy-Chapman electrical double layer model and the 1:1 adsorption model. The 1:1 adsorption model assumes that one Br^- is entrapped by a C16 molecule, and predicts that the concentration of Br^- abruptly decreases below the membrane to a constant value equal to that of the subphase, as illustrated in Fig. 10(a). The Gouy-Chapman model is one of the most efficient models for explaining the adsorption state (Fig. 10(b)). The theoretical edge jump values have been calculated by taking into account the Br^- distributions below the surface as well as the damping of the evanescent wave propagated through the aqueous solution. For a clear comparison, both the experimental values and the Gouy-Chapman predictions were normalized to the values obtained with the 1:1 adsorption model. The dotted black line in Fig. 9 indicates the edge jump values calculated with the 1:1 adsorption model, and the full red line shows the estimation of the Gouy-Chapman model. The results of the surface tension measurements are also shown (green line), and the experimental points (blue) lie between the estimations of these models. The Br^- distribution follows the 1:1 adsorption model for A=180 Å^2, but gradually approaches the Gouy-Chapman model predictions with decreasing *A*. The C16 surface membrane changes from gaseous to a condensed film at A=120 Å^2, where the Br^- distribution almost obeys the Gouy-Chapman model. For A<120 Å^2 the surface tension increases , and the Br^- distribution continues to obey the Gouy-Chapman model. This indicates that the C16 surface membrane is simply compressed without forming a special condensate state with decreasing *A*. Br^- is

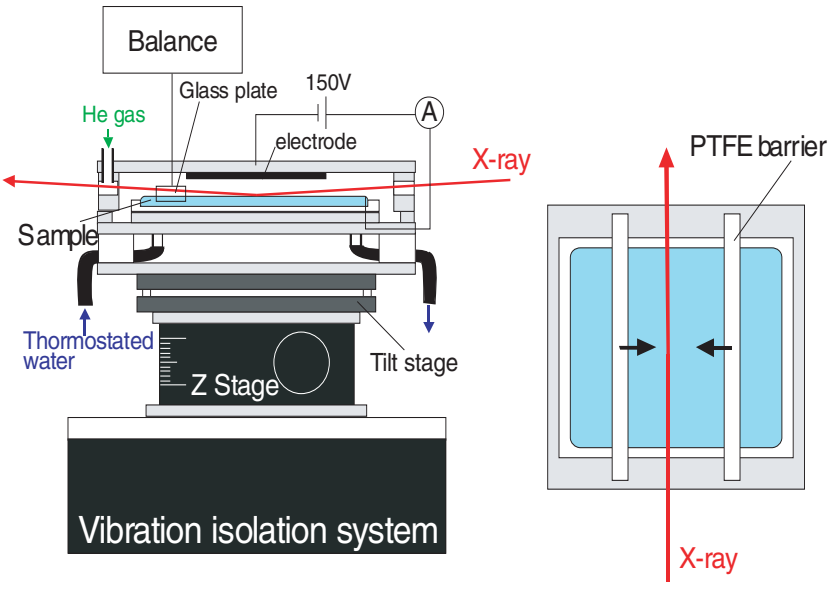

Figure 7
Schematic view of the TRTCY-XAFS cell.

attracted by the positive charges of the C16 molecules, and is adsorbed by C16 molecules at the surface when *A* is large enough to allow the sparse distribution of the surfactant molecules. A decrease in *A* along with a decrease in the Br^--Br^- distance gives rise to an increasing coulombic repulsion and Br^- is released from the C16 surface membrane as a result.

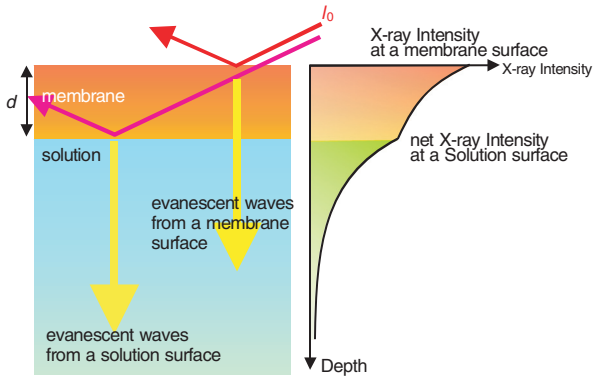

Figure 8
The contribution of the surface membrane to reflection of the incident X-ray.

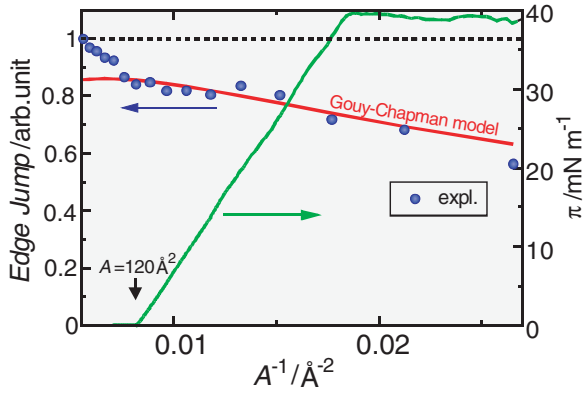

Figure 9
π-A curve (green line) and the edge jump for the C16 surface membrane on 10 mM KBr aqueous solution. Calculated edge jump values from the 1:1 adsorption model (dotted line) and the Gouy-Chapman electrical double layer model (red line). Experimental results (blue circles).

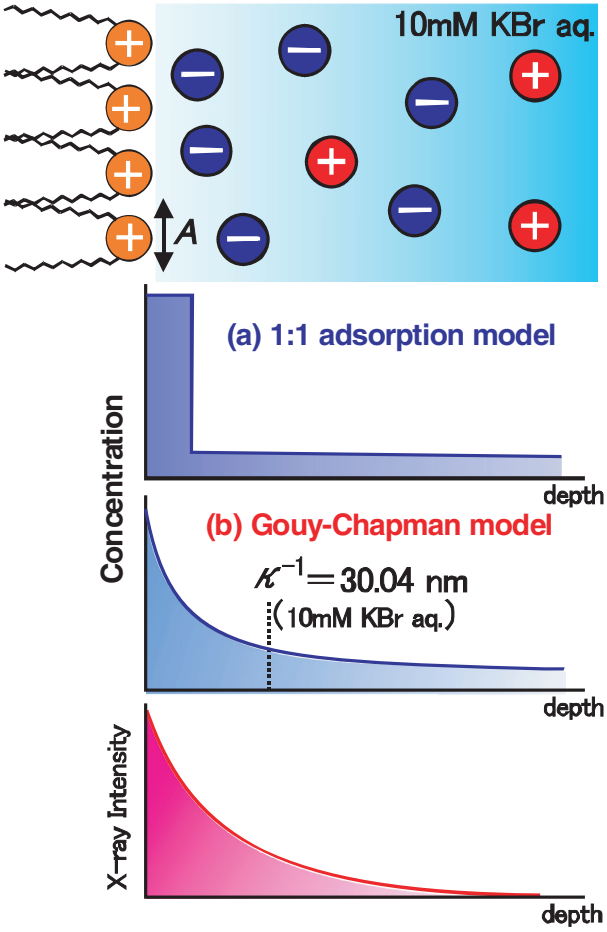

Figure 10
Br^- distribution for (a) the 1:1 adsorption model and (b) the Gouy-Chapman model.

M. Harada and T. Okada (Tokyo Inst. of Tech.)

References

[1] I. Watanabe, H. Tanida, S. Kawauchi, M. Harada and M. Nomura, *Rev. Sci. Instrum.*, **68** (1997) 3307.
[2] M. Harada and T. Okada, *Langmuir,* **20** (2004) 30.
[3] M. Harada and T. Okada, *J. Ion Exchange,* **14**Suppl (2003) 13.
[4] M. Harada, T. Okada and I. Watanabe, *Anal. Sci.,* **18** (2002) 1167.